AGU PUBLICATIONS

JGR

Journal of Geophysical Research: Solid Earth

RESEARCH ARTICLE

10.1002/2016JB013265

Uppermost mantle seismic velocity structure beneath USArray

J. S. Buehler[1] **and P. M. Shearer**[1]

[1] Scripps Institution of Oceanography, University of California, San Diego, La Jolla, California, USA

Key Points:
- USArray and the abundance of quarries in the eastern U.S. allow us to map uppermost mantle lid structure across the contiguous U.S.
- We find a moderate mantle lid velocity gradient for much of the eastern U.S.
- *Pn* anisotropic pattern is not consistent with *SKS* results, suggesting multiple anisotropic layers

Supporting Information:
- Supporting Information S1

Correspondence to:
J. S. Buehler,
jsbuehle@ucsd.edu

Citation:
Buehler, J. S., and P. M. Shearer (2016), Uppermost mantle seismic velocity structure beneath USArray, *J. Geophys. Res. Solid Earth*, *121*, doi:10.1002/2016JB013265.

Received 10 JUN 2016
Accepted 4 DEC 2016
Accepted article online 9 DEC 2016

Abstract We apply *Pn* tomography beneath the entire USArray footprint to image uppermost mantle velocity structure and anisotropy, as well as crustal thickness constraints, beneath the United States. The sparse source distribution in the eastern United States and the resulting longer raypaths provide new challenges and justify the inclusion of additional parameters that account for the velocity gradient in the mantle lid. At large scale, *Pn* velocities are higher in the eastern United States compared to the west, but we observe patches of lower velocities around the New Madrid seismic zone and below the eastern Appalachians. For much of the mantle lid below the central and eastern United States we find a moderate positive velocity gradient. In the western United States, we observe a moderate gradient in the region of the Juan de Fuca subduction zone, but no significant gradient to the south and east of this region. In terms of anisotropy, we find that the *Pn* fast axes generally do not agree with *SKS* splitting orientations, suggesting significant vertical changes in anisotropy in the upper mantle. In particular the circular pattern of the fast polarization direction of *SKS* in the western United States is much less pronounced in the *Pn* results, and in the eastern US the dominant *Pn* fast direction is approximately north-south, whereas the *SKS* fast polarizations are oriented roughly parallel to the absolute plate motion direction.

1. Introduction

At the end of 2013, USArray reached the east coast, completing the grid of uniformly spaced stations at ~70 km spacing across the contiguous United States (http://www.earthscope.org/). A wealth of regional phases from these transportable array stations accumulated over the past 10 years, allowing for continuous imaging of crust and uppermost mantle structure across the USArray station footprint. Here we expand on our *Pn* tomography work for the western United States [*Buehler and Shearer*, 2010, 2014] and image uppermost mantle structure for the entire USArray footprint. We also update our tomography parameterization to include vertical mantle lid velocity gradient terms as suggested by *Phillips et al.* [2007].

Pn arrivals, the first arriving *P* wave at regional distances, have been important for constraining the seismic velocity structure and anisotropy in the mantle lid because they propagate horizontally just below the Moho [e.g., *Hearn*, 1996]. For a narrow depth range at the top of the mantle, they provide good resolution and complement other studies with larger vertical averaging, such as surface wave tomographies and shear wave splitting analysis. In a simple layer over half-space model, *Pn* is critically refracted and propagates with the speed of the faster medium along the boundary. However, such a model is generally only a good approximation at short distances when dealing with real data, as 3-D velocity structure, sphericity of the Earth, and Moho topography cause the *Pn* propagation to be more complicated [e.g., *Cerveny and Ravindra*, 1971; *Zhang et al.*, 2009].

In the tectonically active western United States, regional phases are typically highly attenuated, but the abundance of earthquakes allows us to use many short raypaths. Here the head wave approximation seems justified. In the eastern United States, the events are relatively sparse (and many of them are quarry blasts), but attenuation also tends to be lower [e.g., *Molnar and Oliver*, 1969], so that *Pn* arrivals can be seen to great distances. To increase ray coverage in the east, it is desirable to include longer *Pn* raypaths, but including these longer rays provides new challenges because the *Pn* rays may sample deeper in the mantle and a simple head wave assumption is no longer adequate. To address this, we incorporate additional parameters in the *Pn* tomography that account for the velocity gradient in the mantle lid.

The mantle lid describes the region between the Moho and the lithosphere-asthenosphere boundary, and its thickness varies from a few tens of kilometers up to about 200 km depending on lithospheric structure. A positive vertical velocity gradient in the mantle lid causes the *Pn* rays to bend and interfere, deviating from

that of a pure head wave [*Cerveny and Ravindra*, 1971]. *Zhao* [1993] and *Zhao and Xie* [1993] demonstrated the importance of accounting for vertical mantle lid velocity gradients when working with *Pn* head waves and potential pitfalls of interpreting a positive velocity gradient as azimuthal anisotropy. *Phillips et al.* [2007] then showed how these gradient terms can be added to the *Pn* tomographic setup suggested by *Hearn* [1996]. Velocity gradients will not only influence path and arrival times but also the amplitudes of head waves [*Hill*, 1971]. It was early noted that the regional *Pn* phase amplitudes show large variations between the western and eastern United States [*Evernden*, 1967; *Langston*, 1982], indicating different lithospheric structure.

Pn analysis has previously been attempted in the central and eastern United States [e.g., *Smith and Ekstroem*, 1999; *Zhang et al.*, 2009] with much sparser station coverage, and without the velocity gradient considerations. Here we follow the approach by *Phillips et al.* [2007], but with added parameters accounting for azimuthal anisotropy. This allows us to use larger cutoff distances in the eastern United States, increasing data coverage. It is well known that parameters can trade off in traditional *Pn* tomography. Adding even more free parameters will only amplify this problem. To address this, we perform a series of inversions with an increasing number of model parameters to test the consistency of the imaged structure. First, we assess the character of *Pn* waveforms in different regions of the United States to obtain a broad impression of the nature of *Pn* propagation. Then, we run several *Pn* inversions with different data subsets and assess trade-offs with the anisotropic structure. In addition to uppermost mantle structure, *Pn* tomography also allows us to estimate crustal thickness across the continent. Finally, we discuss the imaged crust and uppermost mantle velocity structure with respect to shear wave splitting and surface wave results.

2. Waveform Stacks and Data Selection

We use regional *Pn* phase data recorded at USArray transportable array stations between April 2004 and July 2014 (Figure 1). Since *Pn* is primarily propagating along the Moho at the *P* wave speed of the uppermost mantle, it will overtake the crustal phase and arrive first at regional distances. Therefore, *Pn* is routinely picked by analysts at the Array Network Facility.

The picks can be downloaded from their website in monthly batches (http://anf.ucsd.edu/tools/events/download.php). We find that the first arrival is not always labeled correctly and hence apply several data processing iterations (similar to the ones described in *Hearn* [1996] and *Buehler and Shearer* [2010]) to correctly identify first arriving *Pn* phases. Given that the crust is generally thicker in the central and eastern United States [e.g., *Chulick and Mooney*, 2002], we use a larger cutoff distance for rays primarily traveling in these regions (250 km, compared to 200 km in the west) because the crossover distance, where *Pn* overtakes the crustal phase, is larger.

Pn has been observed to large distances, but typically, around 1500 to 2000 km deeper turning waves will start to arrive first, as observed in the waveform stacks. However, the change in lithospheric structure between the eastern and western United States leads to different characteristics of regional traveltime branches [e.g., *Walck*, 1985]. Regional phase waveform stacks for four subregions (Figure 2) show not only variations in amplitude (note, for example, how *Sn* is visible in the eastern United States, but not in the two stacks for the west) but also differences in the nature of the *Pn* and the traveltime branches associated with upper mantle triplications. For example, in the southwest it appears that refractions from the 410 km discontinuity start interfering with *Pn* around 15°, but in the east *Pn* arrivals follow a curved path in agreement with a moderate vertical velocity gradient in the mantle lid up to almost 20°. These observations suggest that we must carefully select arrival time picks in order to avoid deeper turning phases and also to have enough data coverage in the eastern United States. In order to avoid triplication refractions in our data set, we use a cutoff distance of 1500 km for the picks with paths predominantly west of 100°W and 2000 km for picks for paths east of 100°W.

This leaves us with about 206,000 *Pn* picks from 12,000 events. Ray coverage is densest in the southwestern United States and sparsest in the northeast (Figure 3). Similar to wanting good azimuthal coverage in order to resolve anisotropy, we desire a good sampling in ray length for each grid cell to image the mantle lid velocity gradient. Shorter rays travel close to the top of the mantle just below the Moho and are relatively insensitive to deeper mantle lid structure. We will not be able to resolve the velocity gradient at locations sampled only by short paths. Figure 3b shows the fraction of rays longer than 1000 km at each location. A few regions, mostly in the west coast, the northern Rocky Mountain area, the coastal Plain, and the Canadian Shield in the east are sampled with predominantly short rays. Velocity gradient structure in these areas is difficult to resolve.

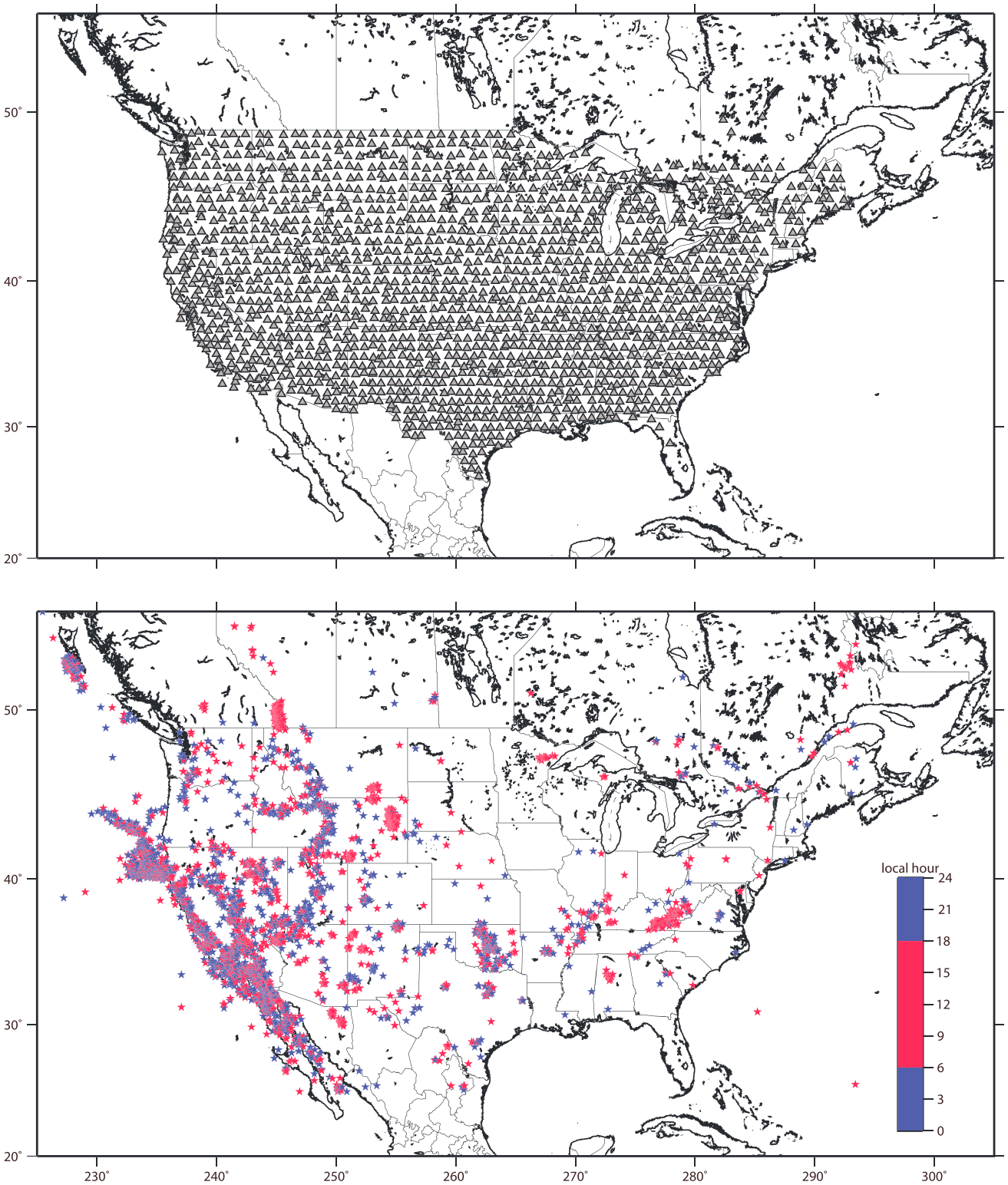

Figure 1. Overview of the stations and events used in this study. The events are marked with blue or red stars, depending on the local time of occurrence (to highlight locations of quarries that mostly operate during the daytime). The stations are indicated with gray triangles.

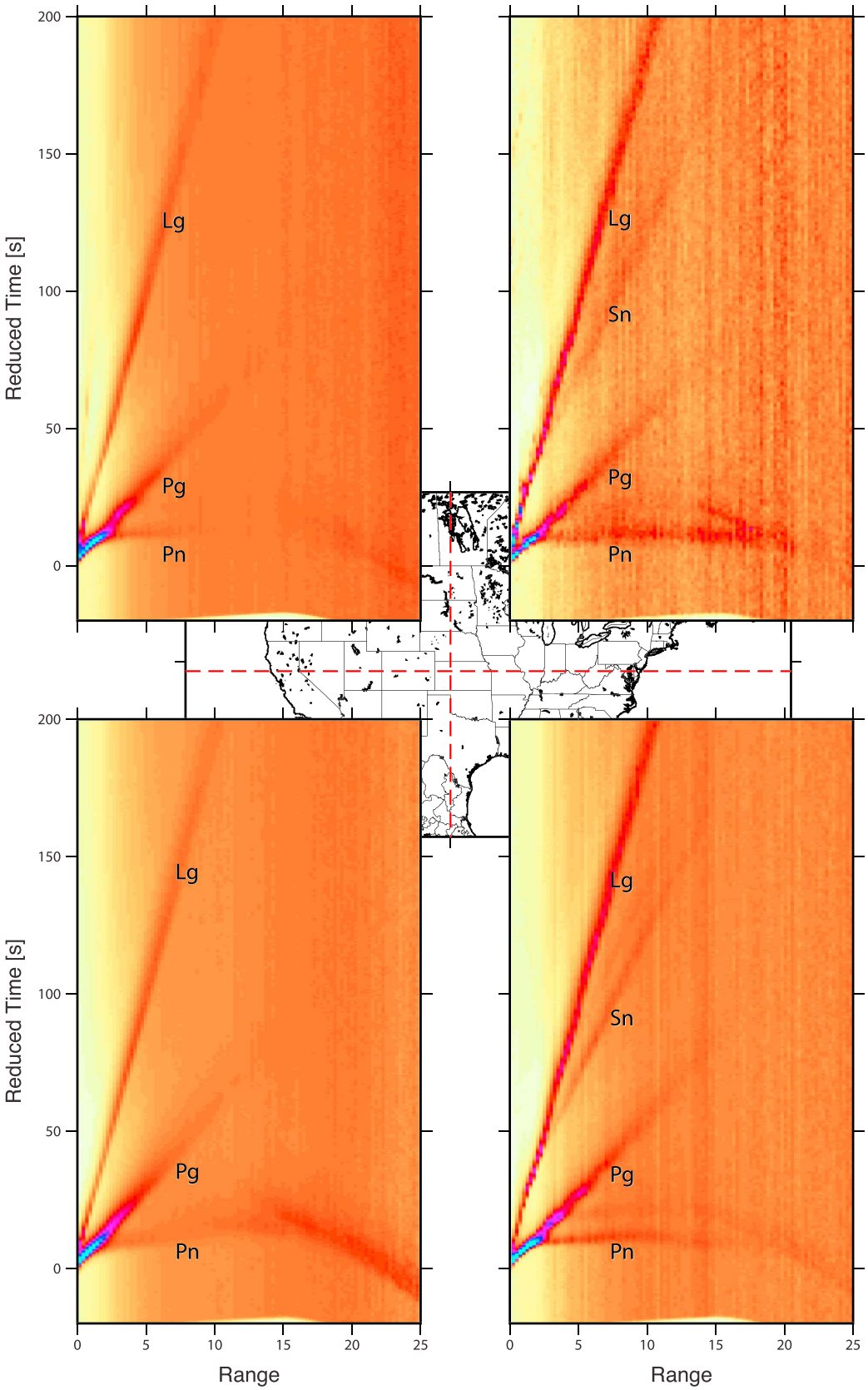

Figure 2. Short-term average to long-term average (STA/LTA) waveform stacks for four different regions, as shown in the background map. Times are adjusted with a reduction velocity of 8.1 km/s.

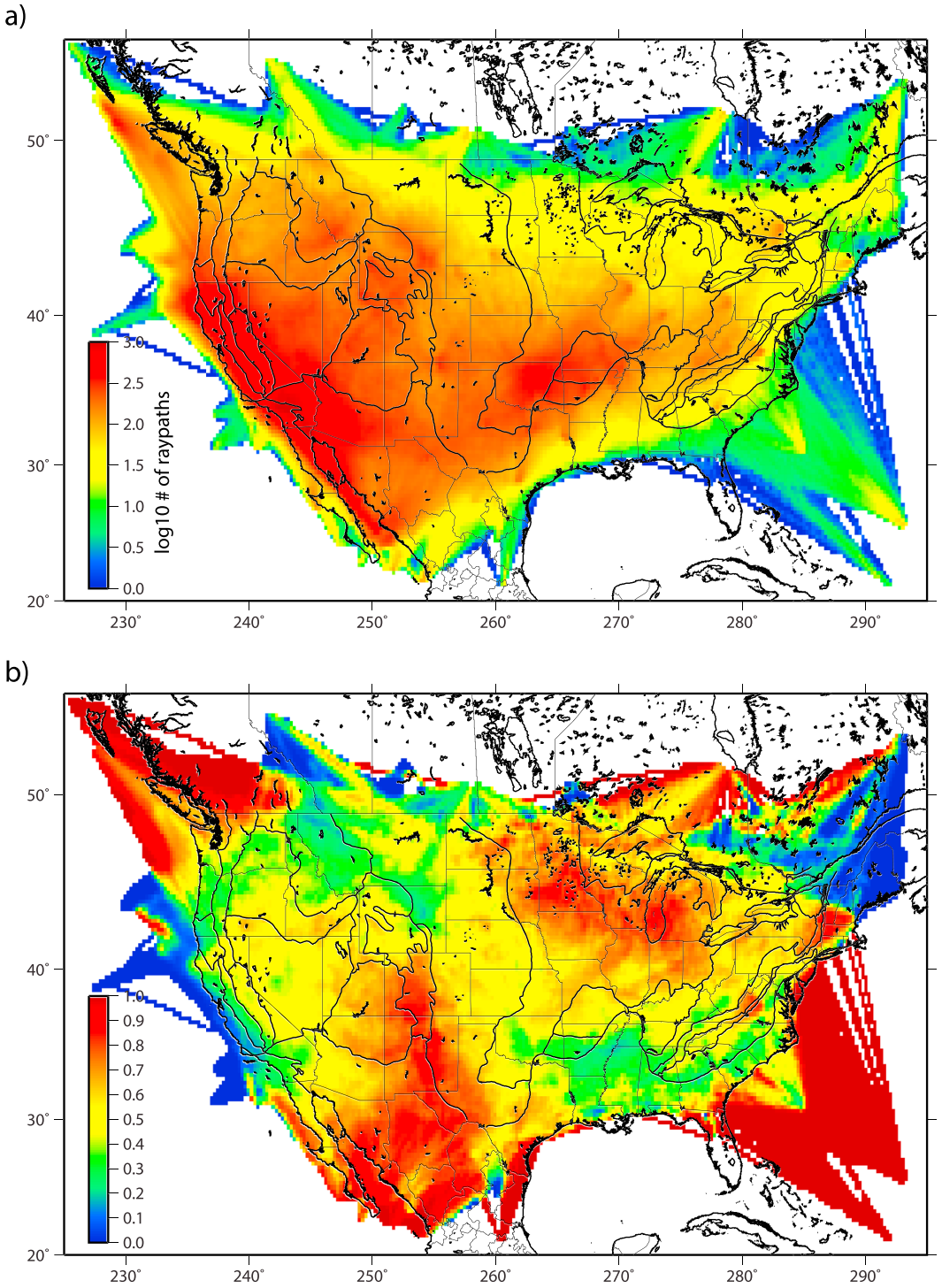

Figure 3. Ray coverage. (a) *Pn* tomography ray coverage. (b) Fraction of rays longer than 1000 km in each cell.

3. *Pn* Tomography

Traditionally, the *Pn* tomography setup is quite simple, using two terms to describe the crustal legs of the raypath and one term that accounts for the mantle portion. Later, *Hearn* [1996] showed how additional terms can be added to account for anisotropy:

$$\delta t_{es} = \delta \tau_e + \delta \tau_s + \Sigma \Delta_{esk} \left(\delta S_k + A_k \cos 2\phi_{esk} + B_k \sin 2\phi_{esk} \right), \quad (1)$$

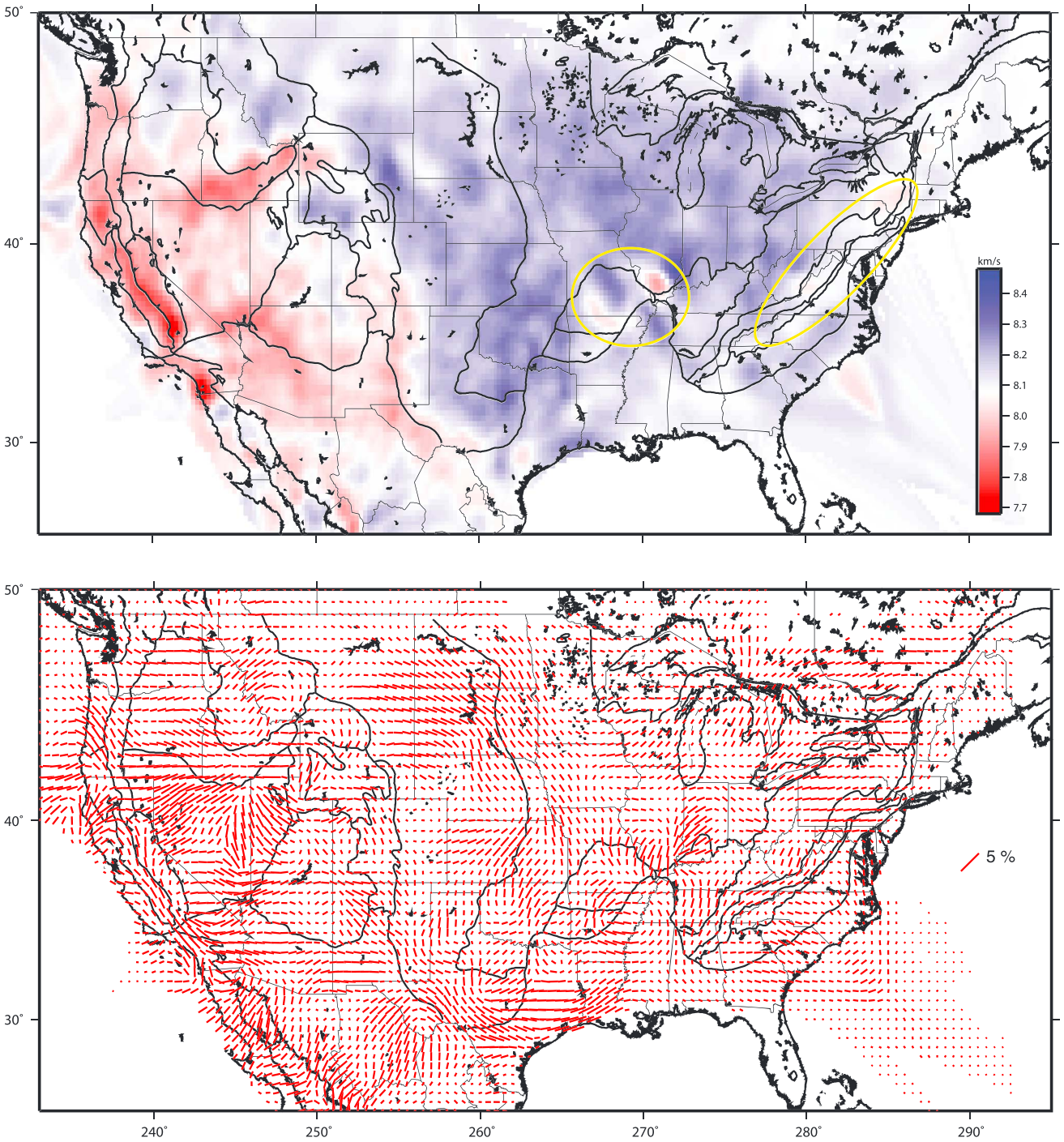

Figure 4. (top) Isotropic and (bottom) anisotropic velocity structure across the USArray footprint without the inclusion of velocity gradient terms. Yellow ovals point out regions of lower velocity in the eastern United States below the New Madrid seismic zone and the Appalachias.

Here $\delta\tau_e$ and $\delta\tau_s$ are event and station time terms absorbing changes in crustal thickness and/or velocities, Δ_{esk} is the ray distance in cell k of the raypath between event e and station s, δS_k is the slowness perturbation in cell k, A_k and B_k are the parameters to describe the azimuthal anisotropy, and ϕ is the back azimuth.

This model describes a head wave sensitive to the velocity structure just below the Moho. However, in the presence of a radial velocity gradient, *Pn* will propagate as a turning wave in the mantle lid [e.g., *Cerveny and Ravindra*, 1971]. *Zhao* [1993] demonstrate how an additional term in the time-term method can account for the change in propagation character. Based on the work by *Zhao* [1993], *Phillips et al.* [2007] then showed how

parameters for the vertical velocity gradient in the mantle lid can be incorporated into two-dimensional *Pn* tomography to solve for lateral variations in radial velocity gradient:

$$\delta t_{es} = \delta\tau_e + \delta\tau_s + \gamma_{es} + \Sigma\Delta_{esk}\left(\delta S_k + A_k \cos 2\phi_{esk} + B_k \sin 2\phi_{esk}\right), \tag{2}$$

where γ_{es} is the gradient term for the raypath between event e and station s:

$$\gamma_{es} = -S_0\Delta_m^3 c^2/24. \tag{3}$$

Here S_0 is the average uppermost mantle velocity, Δ_m is the raypath distance in the mantle between the two piercing points, and c is related to the radial velocity gradient g and a correction for sphericity:

$$c = S_0 g + 0.000158\ \mathrm{km}^{-1}. \tag{4}$$

If the c^2 parameter is allowed to have lateral variations similar to the slowness perturbations, and the path average contributes to the traveltime residual, the resulting *Pn* tomography equation is

$$\delta t_{es} = \delta\tau_e + \delta\tau_s + \Sigma\Delta_{esk}\left(-S_0\Delta_m^2 c_k^2/24 + \delta S_k + A_k \cos 2\phi_{esk} + B_k \sin 2\phi_{esk}\right). \tag{5}$$

Note that because of the Earth's sphericity, rays will still return to the Moho even in the presence of a small negative velocity gradient in the uppermost mantle (i.e., velocity decreasing with depth). However, we do not allow the c^2 parameter to be negative in the inversion, and the sphericity and the average upper mantle velocity determine the smallest possible gradient. *Phillips et al.* [2007] solved for isotropic parameters in addition to the gradient terms. Here we use isotropic, anisotropic, and gradient terms, all of which introduce trade-offs that need to be assessed. For example, in areas with rays mainly from one direction, it will be difficult to distinguish between influences from a vertical gradient or azimuthal anisotropy. In addition, distributions of raypath lengths might influence the gradient parameters, as short rays are not sensitive to the velocity gradient. To navigate these problems, we start by solving for a constant velocity gradient term over the entire region. Next, we subdivide the region into smaller areas and solve the *Pn* tomography problem with a constant velocity gradient for each subregion separately. Finally, we compare these results with a regularized inversion where the gradient is allowed to vary smoothly across the USArray footprint.

4. *Pn* Tomography Results and Discussion

We start our analysis by solving for station and event terms, and a uniform uppermost mantle velocity, to obtain a first-order estimate of Moho topography and average uppermost mantle velocity in the model region. We obtain a best fitting *Pn* velocity of 8.1 km/s and a RMS residual of 0.98 s. Using these results, we estimate the locations of the mantle pierce points, assuming the rays obey Snell's law and a constant crustal velocity of 6.3 km/s, for our 2-D tomography.

First, we solve for isotropic and anisotropic parameters only (Figure 4). Increasing the model region and adding more data in the east does not much influence the isotropic velocity structure in the western United States published in our previous papers [e.g., *Buehler and Shearer*, 2014], although it does have an effect on the amplitudes because of damping regularization toward the average velocity across the continent. In the eastern United States, we obtain the slowest *Pn* velocities below the Appalachian Range, and near the New Madrid seismic zone, at the northern boundary of the Mississippi embayment. *Chen et al.* [2014] map similar low-velocity anomalies around the New Madrid Seismic Zone at 40 km depth, and *Schmandt and Lin* [2014] also image lower velocities below the central and northern Appalachian at 60–100 km depth. As discussed in *Schmandt and Lin* [2014], the location of the low-velocity anomaly below the central Appalachian Range coincides approximately with a young (~47 Ma) localized magmatic event along the eastern North American margin [*Mazza et al.*, 2014]. The cause for volcanism under the Appalachian Range is up for debate. *Schmandt and Lin* [2014] prefer the explanation of lithospheric downwelling instead of plume-related magmatism from passage over a hot spot [*Chu et al.*, 2013] because of their small and very localized anomaly at 75 km depth, which only widens at depths around 200 km, compared to a more elongated long velocity region that would be expected from a hot spot track. Our *Pn* results suggest that low-velocity anomaly has greater lateral spread at the top of the mantle compared to their teleseismic body wave tomography, but we also do not find clear evidence for a continuous track.

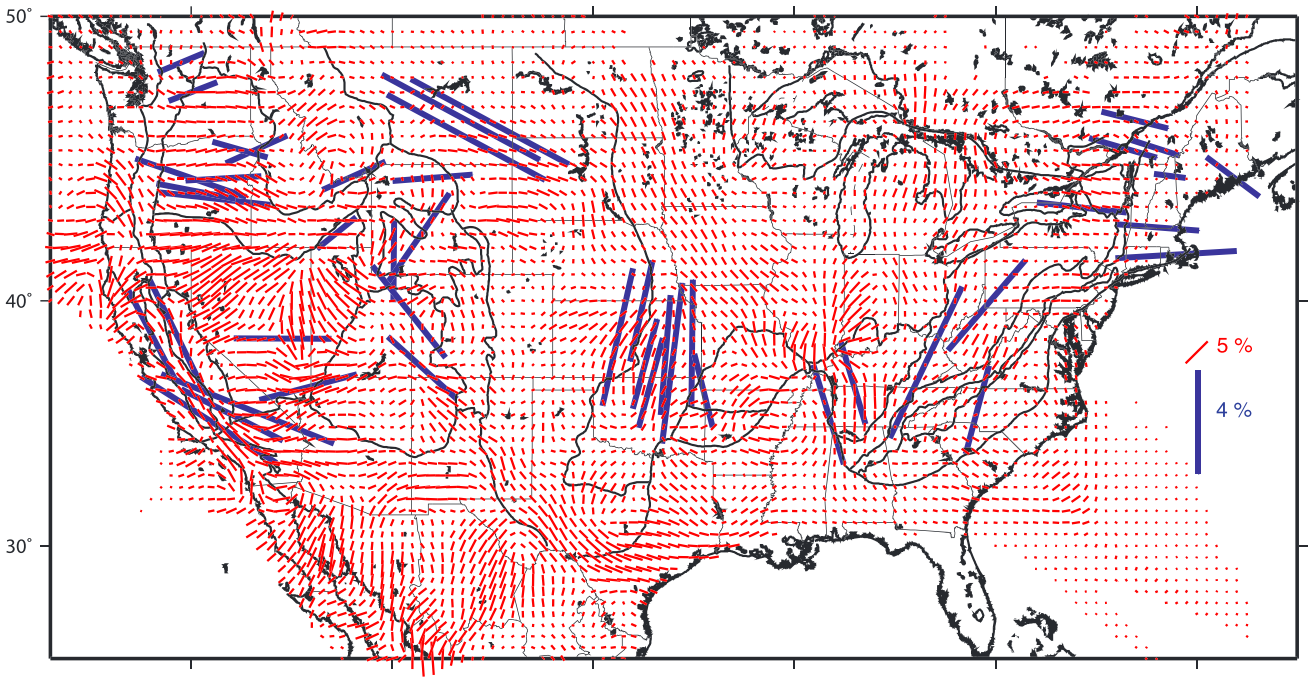

Figure 5. Our *Pn* fast axes (red) compared to *Pn* fast directions from an earlier study by *Smith and Ekstroem* [1999] (blue, note the different scale). Some of the redundant measurements from *Smith and Ekstroem* [1999] are omitted for imaging clarity.

Similar to the western United States, azimuthal anisotropy appears to be very heterogenous in the eastern United States, unlike shear wave splitting results that show predominantly fast polarization directions in accordance with the present absolute plate motion of the North American plate [e.g., *Fouch et al.*, 2000; *Hongsresawat et al.*, 2015]. A combined surface wave and shear wave splitting study by *Yuan et al.* [2011] shows mostly north-south oriented fast axes at 150 km depth (lithospheric contribution), and northeast-southwest oriented axes at 250 km, in agreement with the absolute plate motion direction. Our *Pn* anisotropy results are largely consistent with an earlier *Pn* study by *Smith and Ekstroem* [1999], which shows relatively strong anisotropy with northwest-southeast fast directions in the northern Great Plains, rotating to northeast-southwest further south (Figure 5). Similar to *Smith and Ekstroem* [1999], we also image fast directions parallel to the Appalachian front and north-south fast directions beneath the Central Plains. As noted in *Deschamps et al.* [2008], shear wave splitting and *Pn* results appear to show similar fast directions between the Appalachian and Grenville provinces but disagree to the south and north of this region, suggesting multiple anisotropic layers in the crust and upper mantle.

Adding a uniform velocity gradient term to the tomography does not affect the lateral isotropic and anisotropic structure results very much. The best fitting velocity gradient is 0.001 s^{-1} across the continent. Solving for a single gradient results in only a slightly better data fit (root-mean-square (RMS) residual of 0.70 s and variance reduction of 49%, compared to a RMS residual of 0.71 s and 47% variance reduction without a gradient term). Next, we allow the gradient terms to vary on a 2-D grid (Figure 6), resulting in additional variance reduction (RMS residual of 0.69 s, 51% variance reduction). Although this might appear to be a relatively small improvement in fit, it should be noted that only a relatively small fraction of raypaths are influenced by the gradient terms by a large amount, as the majority of raypaths are short. If we only consider the residuals with a gradient contribution of larger than 0.8 s (according to the model), the variance reduction is 75%, compared to 63% without gradient terms for the same paths. Residual-distance plots show that the inclusion of gradient terms removes the sloping of the residuals at greater distances (see supporting information for details). The remaining variation in the data that we cannot fit with our model parameterization appears to be mostly at shorter ranges. At shorter distances, the crustal contribution to the residuals is larger relative to longer raypaths that spend larger amounts of time in the upper mantle, and the remaining data variation might be a combination of picking error (for example, energy refracted in the lower crust might arrive very close to the *Pn* arrival) and azimuthal velocity variations in the crust.

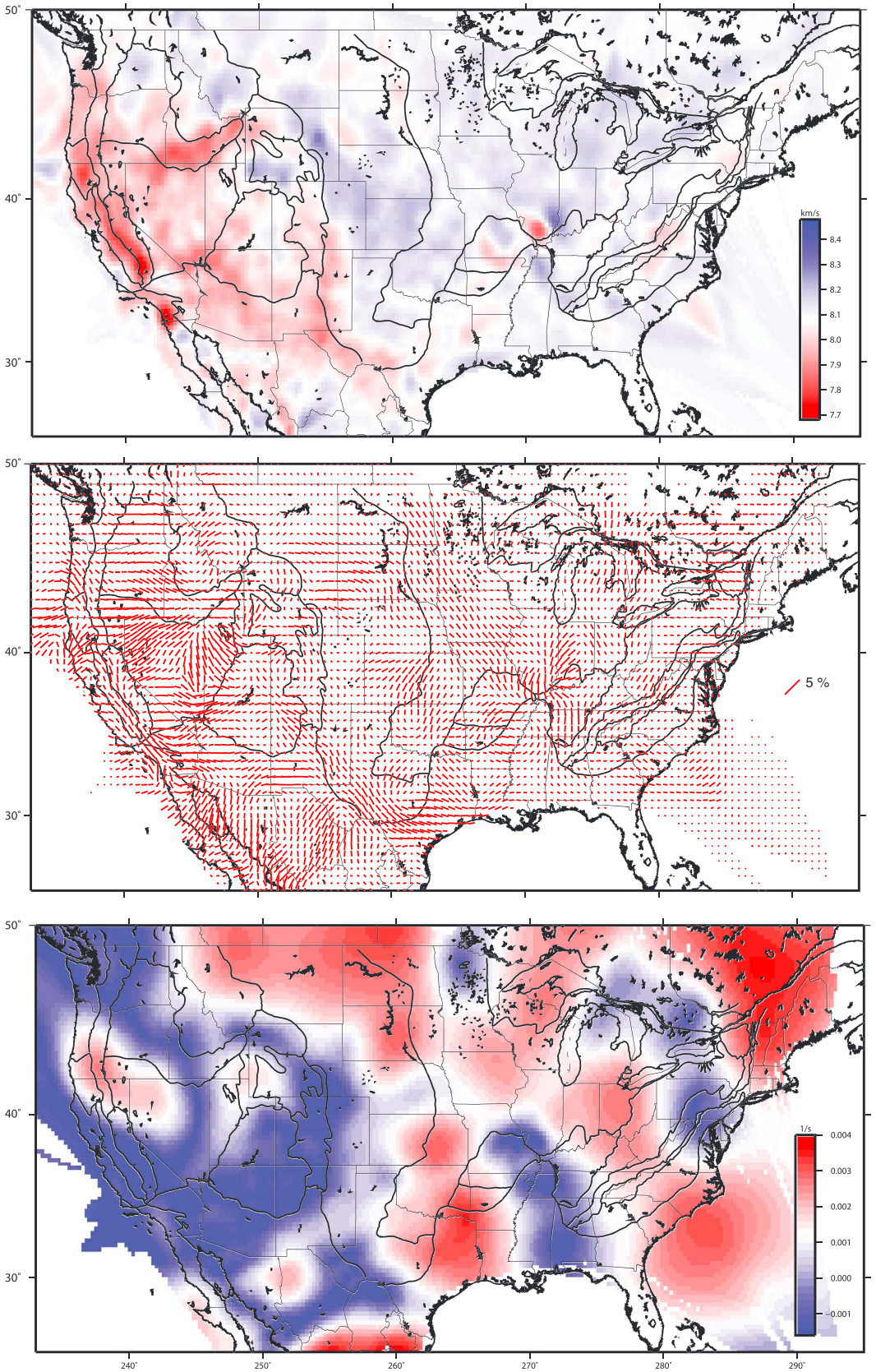

Figure 6. (top) Uppermost mantle isotropic (top), (middle) anisotropic, and (bottom) vertical velocity gradient structure across the USArray footprint.

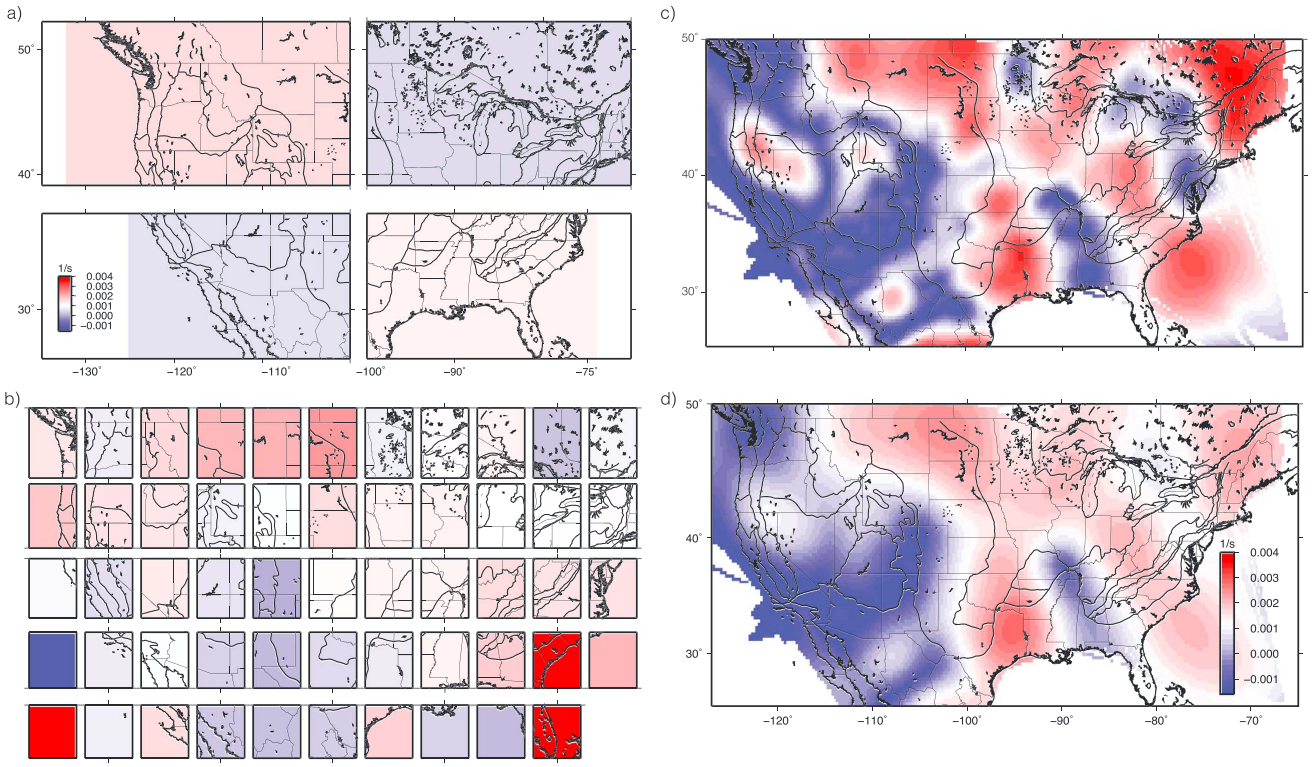

Figure 7. Vertical mantle lid velocity gradient. (a) Uniform gradient in four regions from four separate *Pn* inversions. (b) Uniform gradient term in subregions across the continent. (c) The 2-D *Pn* tomography gradient image. (d) Heavily smoothed gradient terms.

Overall, introducing a lateral varying gradient term lowers the high velocities in the central and eastern United States, presumably since now we account for these deeper turning rays sampling higher velocities. As a result, the regions with lower velocities in the east become more visible, especially the lower velocity zone below the Appalachias, in the Coastal Plain, and around the New Madrid seismic zone. The introduction of gradient terms lowers the magnitude of the anisotropy, especially in the central Great Plain, but does not affect the patterns. Similar to the isotropic structure, at large scale the vertical gradient structure appears different east and west of the Rocky Mountain front. The inversion shows moderate velocity gradients for the central and much of the eastern parts of the USArray footprint. In the western United States we observe a patch of moderate gradient in the broad area of the Juan de Fuca subduction zone.

A uniform velocity gradient across the continent does not appear reasonable given the difference in lithospheric structure and tectonic history between the western and eastern United States. However, allowing the gradient to vary too much laterally might cause trade-offs or large variabilities along a single ray. We attempt to test the reliability of the gradient structure with both heavier regularization and separate *Pn* inversions for smaller regions, only allowing for a uniform gradient term. Figure 7a shows the results for four separate *Pn* tomographies for the four regions we previously produced waveform stacks. In each of the inversions, using only stations and events within these subregions, we only allow for a uniform gradient term. We obtain a moderate gradient in the northwest and the southeast, but not in the southwest and northeast. This could suggest that the strong gradient imaged in the Canadian shield and northeastern United States (Figure 6) is an artifact of sparse data coverage and regularization. That this region is mostly sampled by short rays makes the imaged moderate gradient also less likely to be accurate.

Since this division into four rectangles is somewhat arbitrary, we next move the rectangles across the USArray footprint, solving for *Pn* parameters in each subregion separately. In Figure 7b, we plot the resolved velocity gradient at the center of each 20 by 15° area in longitude and latitude. Similar to the regular 2-D tomography (again displayed in Figure 7c for comparison), we obtain moderate gradients for the subduction region in the west and much of the central and eastern parts of the region. The biggest inconsistencies occur in the southeastern part of the model area, where, for example, the 2-D tomography shows a reduced gradient below

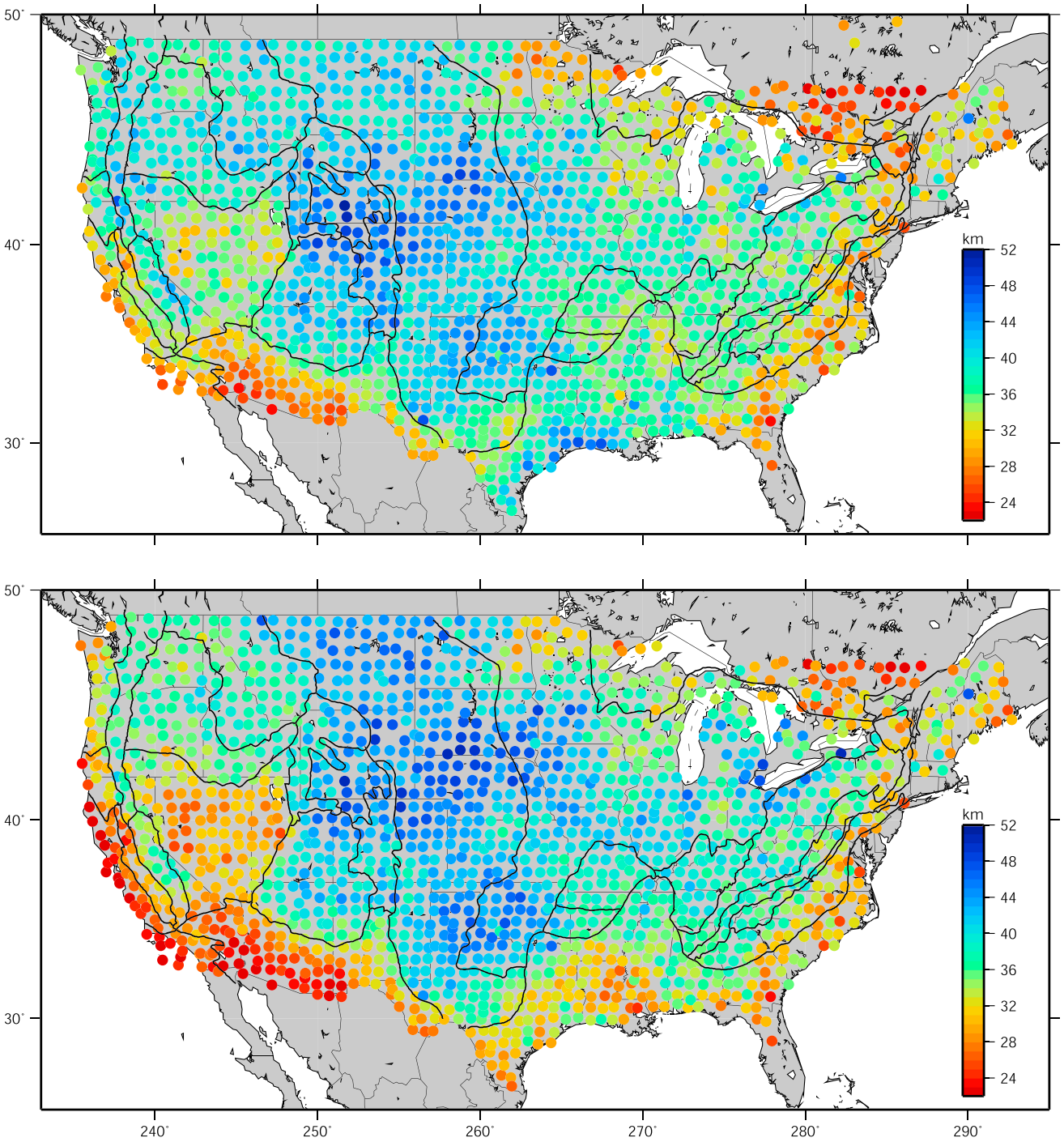

Figure 8. (a) Crustal thickness estimates from *Pn* station time terms, assuming a constant crustal velocity of 6.3 km/s. (b) Crustal thickness estimates from *Pn* station time terms and the crustal velocities from *Shen and Ritzwoller* [2016].

much of the Mississippi embayment and the New Madrid rift complex. Figure 3b shows that the raypaths crossing here are mostly short. It is possible that here the 2-D tomography is more accurate than the separate subregion inversions, because by dividing the data sets, we eliminate the few long paths from earthquakes in the Gulf of California. It should be possible to gain further insight into the vertical velocity structure of the mantle lid by considering *Pn* amplitude information [*Nielsen et al.*, 2003; *Sereno*, 1989]. We have not explored this in detail but did perform some tests that confirmed that regions with higher velocity gradients in our model produce higher *Pn* amplitudes and that these amplitude variations are roughly consistent with those

predicted using synthetic seismogram modeling (see supporting information for details). Future work could explore the addition of *Pn* amplitude measurements to further constrain the vertical velocity gradient in the mantle lid.

Most of the areas with positive velocity gradients correspond to regions of the North American craton, with lithosphere-asthenosphere boundary depth larger than ~100 km [*Yuan et al.*, 2011; *Artemieva*, 2009], increased effective elastic thickness [*Kirby and Swain*, 2009], and low surface heat flow [*Blackwell et al.*, 2011]. Because of these observations, it seems likely that temperature is the dominant effect controlling the mantle lid gradient. As discussed in *Tittgemeyer et al.* [2000] and *Faul and Jackson* [2005], a positive mantle lid gradient is not straightforward to explain for the average lithosphere: Typical geotherms generally seem to lead to negative lid gradients, as the temperature gradient is high in the lithosphere, offsetting the increased pressure effect that would lead to increased velocities for unaltered compositions, causing velocities to decrease. For this reason, and the limited ability of *Pn* to resolve negative gradients and smaller scale structure, it is difficult to further distinguish among temperature effects causing negative gradients (such as lithospheric root removal). However, positive mantle lid gradients only seem possible in areas with low mantle heat flow, such as stable regions of continents, and can provide an additional constraint for thermal modeling.

Finally, we use the *Pn* station time terms to estimate crustal thickness. For the estimates imaged in Figure 8a we assume a constant crustal velocity of 6.3 km/s. We image the thickest crust in central North America and the shallowest crust in the southern Basin and Range, the southeastern part of the Coastal Plains, and the southern Canadian Shield. The thick crust imaged in southern Texas is likely an artifact of using a constant crustal velocity. The crustal velocity is very low in the Mississippi Embayment [e.g., *Bensen et al.*, 2009], likely resulting in overly high thickness estimates in this region. To test this, we use the crustal velocity model of *Shen and Ritzwoller* [2016] to convert our station time terms to thickness estimates (Figure 8b). This results in lower crustal thickness along the coasts and the Great Basin area, and a thicker crust throughout the Great Plains. The large-scale features look very similar to *Shen and Ritzwoller* [2016]'s own crustal thickness model—derived from a combination of surface wave, receiver function, and ambient noise analysis—with the exception that our crust is thinner below the Appalachians.

5. Conclusions

USArray station coverage and the abundance of quarries in the eastern United States allow us to map uppermost mantle lid structure across the contiguous United States. We accommodate the different data character and sparser distribution in the eastern United States with additional parameters to account for the vertical mantle lid gradient in our *Pn* tomography. We find that the mantle lid structure differs between the western and eastern United States. The change from low to moderate mantle lid gradients corresponds roughly with the region between the Rocky Mountains and the Great Plains that marks the boundary between the slow *Pn* velocities in the west and the higher velocities in the east. This change in mantle lid gradient structure is also consistent with observed changes in *Pn* amplitude across different profiles. The anisotropic patterns seem to be of smaller scale and are generally not consistent with shear wave splitting results, suggesting multiple anisotropic layers in the crust and upper mantle.

Acknowledgments
We thank the Associate Editor and two reviewers for their constructive comments. This research was supported by National Science Foundation grant EAR-1358510. All data are available from the Array Network Facility (http://anf.ucsd.edu/, last accessed on May 2016). The models are available for download via the IRIS Earth Model Collaboration at http://ds.iris.edu/ds/products/emc/. References *Burdick and Helmberger* [1978] and *Kennett* [2009] refer to our supporting information.

References

Artemieva, I. M. (2009), The continental lithosphere: Reconciling thermal, seismic, and petrologic data, *Lithos*, *109*(1), 23–46.
Bensen, G., M. Ritzwoller, and Y. Yang (2009), A 3-D shear velocity model of the crust and uppermost mantle beneath the United States from ambient seismic noise, *Geophys. J. Int.*, *177*(3), 1177–1196.
Blackwell, D., M. Richards, Z. Frone, A. Ruzo, R. Dingwall, and M. Williams (2011), Temperature-at-depth maps for the conterminous US and geothermal resource estimates, *GRC Trans.*, *35*, GRC1029452.
Buehler, J. S., and P. M. Shearer (2010), *Pn* tomography of the western United States using USArray, *J. Geophys. Res.*, *115*, B09315, doi:10.1029/2009JB006874.
Buehler, J. S., and P. M. Shearer (2014), Anisotropy and *Vp*/*Vs* in the uppermost mantle beneath the western United States from joint analysis of *Pn* and *Sn* phases, *J. Geophys. Res. Solid Earth*, *119*, 1200–1219, doi:10.1002/2013JB010559.
Burdick, L. J., and D. V. Helmberger (1978), The upper mantle *P* velocity structure of the western United States, *J. Geophys. Res.*, *83*(B4), 1699–1712.
Cerveny, V., and R. Ravindra (1971), *Theory of Seismic Head Waves*, Univ. of Toronto Press, Toronto, Ontario.
Chen, C., D. Zhao, and S. Wu (2014), Crust and upper mantle structure of the New Madrid Seismic Zone: Insight into intraplate earthquakes, *Phys. Earth Planet. Int.*, *230*, 1–14.
Chu, R., W. Leng, D. V. Helmberger, and M. Gurnis (2013), Hidden hotspot track beneath the eastern United States, *Nat. Geosci.*, *6*(11), 963–966.
Chulick, G. S., and W. D. Mooney (2002), Seismic structure of the crust and uppermost mantle of North America and adjacent Oceanic Basins: A synthesis, *Bull. Seismol. Soc. Am.*, *92*(6), 2478–2492, doi:10.1785/0120010188.

Deschamps, F., S. Lebedev, T. Meier, and J. Trampert (2008), Azimuthal anisotropy of Rayleigh-wave phase velocities in the east-central United States, *Geophys. J. Int.*, *173*(3), 827–843.
Evernden, J. F. (1967), Magnitude determination at regional and near-regional distances in the United States, *Bull. Seismol. Soc. Am.*, *57*(4), 591–639.
Faul, U. H., and I. Jackson (2005), The seismological signature of temperature and grain size variations in the upper mantle, *Earth Planet. Sci. Lett.*, *234*(1–2), 119–134.
Fouch, M. J., K. M. Fischer, E. M. Parmentier, M. E. Wysession, and T. J. Clarke (2000), Shear wave splitting, continental keels, and patterns of mantle flow, *J. Geophys. Res.*, *105*(B3), 6255–6275.
Hearn, T. M. (1996), Anisotropic *Pn* tomography in the western United States, *J. Geophys. Res.*, *101*(B4), 8403–8414.
Hill, D. P. (1971), Velocity gradients and anelasticity from crustal body wave amplitudes, *J. Geophys. Res.*, *76*(14), 3309–3325.
Hongsresawat, S., M. P. Panning, R. M. Russo, D. A. Foster, V. Monteiller, and S. Chevrot (2015), USArray shear wave splitting shows seismic anisotropy from both lithosphere and asthenosphere, *Geology*, *43*, 667–670, doi:10.1130/G36610.1.
Kennett, B. (2009), *Seismic Wave Propagation in Stratified Media*, ANU Press, Canberra.
Kirby, J. F., and C. J. Swain (2009), A reassessment of spectral Te estimation in continental interiors: The case of North America, *J. Geophys. Res.*, *114*, B08401, doi:10.1029/2009JB006356.
Langston, C. A. (1982), Aspects of *Pn* and *Pg* propagation at regional distances, *Bull. Seismol. Soc. Am.*, *72*(2), 457–471.
Mazza, S. E., E. Gazel, E. A. Johnson, M. J. Kunk, R. McAleer, J. A. Spotila, M. Bizimis, and D. S. Coleman (2014), Volcanoes of the passive margin: The youngest magmatic event in eastern North America, *Geology*, *42*, 483–486, doi:10.1130/G35407.1.
Molnar, P., and J. Oliver (1969), Lateral variations of attenuation in the upper mantle and discontinuities in the lithosphere, *J. Geophys. Res.*, *74*(10), 2648–2682.
Nielsen, L., H. Thybo, I. B. Morozov, S. B. Smithson, and L. Solodilov (2003), Teleseismic P_n arrivals: Influence of mantle velocity gradient and crustal scattering, *Geophys. J. Int.*, *152*(2), F1–F7, doi:10.1046/j.1365-246X.2003.01873.x.
Phillips, W. S., M. L. Begnaud, C. A. Rowe, L. K. Steck, S. C. Myers, M. E. Pasyanos, and S. Ballard (2007), Accounting for lateral variations of the upper mantle gradient in P_n tomography studies, *Geophys. Res. Lett.*, *34*, L14312, doi:10.1029/2007GL029338.
Schmandt, B., and F. Lin (2014), P and S wave tomography of the mantle beneath the United States, *Geophys. Res. Lett.*, *41*, 6342–6349, doi:10.1002/2014GL061231.
Sereno, T. J. (1989), Numerical modeling of Pn geometric spreading and empirically determined attenuation of Pn and Lg phases recorded in eastern Kazakhstan, Tech. Rep., Sci. Appl. Int. Corp., Tysons Corner, Va.
Shen, W., and M. H. Ritzwoller (2016), Crustal and uppermost mantle structure beneath the United States, *J. Geophys. Res. Solid Earth*, *121*, 4306–4342, doi:10.1002/2016JB012887.
Smith, G. P., and G. Ekstroem (1999), A global study of P_n anisotropy beneath continents, *J. Geophys. Res.*, *104*(B1), 963–980.
Tittgemeyer, M., F. Wenzel, and K. Fuchs (2000), On the nature of P_n, *J. Geophys. Res.*, *105*(B7), 16,173–16,180.
Walck, M. C. (1985), The upper mantle beneath the north-east Pacific rim: A comparison with the Gulf of California, *Geophys. J. R. Astron. Soc.*, *81*(1), 243–276.
Yuan, H., B. Romanowicz, K. M. Fischer, and D. Abt (2011), 3-D shear wave radially and azimuthally anisotropic velocity model of the North American upper mantle, *Geophys. J. Int.*, *184*(3), 1237–1260.
Zhang, Q., E. Sandvol, and M. Liu (2009), Tomographic *Pn* velocity and anisotropy structure in the central and eastern United States, *Bull. Seismol. Soc. Am.*, *99*(1), 422–427, doi:10.1785/0120080246.
Zhao, L.-S. (1993), Lateral variations and azimuthal isotropy of P_n velocities beneath Basin and Range Province, *J. Geophys. Res.*, *98*(B12), 22,109–22,122.
Zhao, L.-S., and J. Xie (1993), Lateral variations in compressional velocities beneath the Tibetan Plateau from P_n traveltime tomography, *Geophys. J. Int.*, *115*(3), 1070–1084, doi:10.1111/j.1365-246X.1993.tb01510.x.